Effect of Co-doping on Hydrophilic and Photoelectric Properties of Co-dopedtitania Nanoparticles as Composition of Electrode Modifier

Nasrin Ahmadi [1], Ali Nemati [2,*], Mojtaba Bagherzadeh [3]

[1] Department of Materials Engineering, Science and Research Branch, Islamic Azad University, Tehran, Iran
[2] Department of Materials Science & Engineering, Sharif University of Technology, Tehran, Iran
[3] Reactor and Nuclear Safety School, Nuclear Science and Technology Research Institute, 81465-1589, Isfahan, Iran

ARTICLE INFO

Article history:

Received 20 August 2019
Accepted 7 November 2019
Available online 25 December 2019

Keywords:

Doped titania
Nitrogen
Cerium
Photoelectric
Hydrophilic

ABSTRACT

In this study, nitrogen and cerium co-doped titanium dioxide nanoparticles were prepared by sol-gel method and were calcined in air at550 °C for 2 hours. Then, the surface glassy carbon electrode was modified and coated with synthesized nanoparticles. The crystalline structure of the nanoparticles was characterized by X-ray diffraction (XRD). The topography, surface roughness and particle size distribution of the coatings were investigated by atomic force microscopy (AFM). Photoelectric properties such as the changes of the absorption edges and band gap values of the nanoparticles were studied by diffuse reflectance spectra (DRS). The hydrophilic property of the coatings was also measured by a contact angle device. In all of the analyses, the effect of nitrogen doping amount on the characteristics of N, Ce co-doped titania samples was investigated. According to the results, the band gap of the co-doped titania samples relative to that of pure titania has been decreased (from ≅ 3.21 eV to ≅ 2.78 eV) and their surface hydrophilicity has been improved (from 1.01 (deg.min^{-1}) to 1.60 (deg.min^{-1})). Among the samples the co-doped titania contains the ratio of Ce/Ti: 1% and N/Ti: 0.25%, has the highest amount of anatase phase (≅ 93.1%), the lowest agglomeration at the surface, the smallest band gap energy (≅ 2.78 eV) and the highest photo-induced super-hydrophilicity (hydrophilicizing rate: 1.60 (deg.min^{-1})).

1-Introduction

Recently, titania has received much attention, since it has some outstanding properties such as good chemical and physical stability, non-toxicity, low price, high photocatalytic activity, special hydrophilic and photoelectric properties [1-3]. TiO_2 has been used in many fields, for instance, photocatalyst, antibacterial, hydrophilic materials and electrode modifiers of sensors [4-7]. In recent years, electrochemical and photoelectrochemical biosensors have been designed based on surface modification of electrodes by semiconductors such as titania to detect biomolecules [6, 7]. In general, the titania has a wide band gap (≅ 3.2 eV) and shows photocatalytic activity only under UV light irradiation. On the other hand, in titania, the lifetime of photo-excited electron-hole pair is short and charge carriers recombination occurs, which lead to the reduction of the photoelectric properties of TiO_2 [2, 3]. Furthermore, UV light damages biomolecules and it's not applicable

* Corresponding author:
E-mail address: nemati@sharif.edu

for designing an electrochemical and photoelectrochemical sensing of biomolecules. There are various ways to improve the performance of titania under visible light, such as the doping with metallic, non-metallic and rare earth elements, the connection of semiconductors to each other and dye-sensitization [8-12].

In this study, nitrogen and cerium dopants were selected to improve titania performance under visible irradiation. Cerium doping has been received significant interest due to its specific 4f orbitals' electrons configuration, the redox couple Ce^{3+}/Ce^{4+}, the trapping of electrons by this oxidation-reduction pair and as a result the increasing of lifetime of photo-excited electron-hole pair [13-15]. And doping of nitrogen into titania lattice was reported, which can shift the band gap and absorption edge to lower energy levels. In this regard, due to contribution of p orbitals into the band gap narrowing by mixing with oxygen 2p orbitals [15-17].

In this study, to improve the hydrophilic and photoelectric properties of titania nanoparticles, nitrogen and cerium were co-doped into titania structure. Pure and N, Ce co-doped titania samples were synthesized via a sol–gel method. Then, photo-induced hydrophilicities and photoelectric activities of co-doped titania samples were investigated and compared with the pure titania sample with focus upon the effect of nitrogen content on the photo activities. Finally, the optimal sample was selected to modify electrode surface and to improve its performance for photoelectrochemical applications.

2- Experimental procedure

2-1- Materials and equipment

Tetra-n-butyl orthotitanate (98%), nitric acid (63%) and ethanol absolute were purchased from Merck®. Urea (99.5%) and cerium (III) nitrate hexahydrate (99.5%) were purchased from Acros® and Alfa aesar®, respectively. The X-ray diffraction (XRD) was used with Cu K_α radiation (λ=0.1541 nm) at a scan rate of 0.05 $2\theta s^{-1}$, (Philips PW3040). The topography, surface roughness and particle size distribution of the samples were investigated by atomic force microscopy in contact mode (AFM: Auto probe, CP model). Ultraviolet-visible light diffuse reflectance spectra (DRS) were applied using a UV-Vis spectrophotometer (Jasco V570 Accessory ARN 475) within the wavelength range of 200-800 nm. Contact angle measurements were by the sessile drop method by a contact angle device (OCA 15 puls, Data Physics). Water droplets were placed at three different positions for each sample, and the average values were adopted as the contact angles.

2-2- Synthesis of pure titania and N, Ce co-doped titania

In this investigation, pure and N, Ce co-doped titania nanoparticles were synthesized by sol-gel method [15]. For this purpose, the constant amount of cerium(III) nitrate hexahydrate besides different amounts of urea were dissolved in absolute by the Ce/Ti doping ratio: 1% and N/Ti doping ratio of 0, 0.25, 0.5, 1 and 2%, respectively. The pervious solution was added into a tetra-n-butyl orthotitanate solution in absolute ethanol. Then, the resulting transparent sol was peptized at room temperature for about 48 hours. Then, the mixture of ethanol, nitric acid and deionized water were added drop wise to the resulting solution until the sol was changed to gel. The gel was air dried at 110 ℃ for 1 hour. Finally, it was calcined at 550 ℃ under air atmosphere for 2 hours at maximum temperature [15]. It is noteworthy that pure titania nanoparticles (T sample) were prepared via the same manner using tetra-n-butyl orthotitanate, without cerium (III) nitrate hexahydrate and urea in the composition. The pure and N, Ce co-doped titania nanoparticles were (N-C-T samples) were prepared.

2-3- Surface coating of the electrodes

In the next step, to modification of the electrochemical and photoelectrochemical electrodes, a glassy carbon electrode (GCE) was polished by using alumina powder and then rinsed by sonication in ethanol and deionized water for 5 min. 10 mg the powder (pure and N, Ce co-doped titania) dispersed in 5 ml ethanol and deionized water and then 20 µl of the suspension was coated onto the GCE surface and dried at room temperature to construction of the modified and coated electrode.

2-4- List of symbols

Table 1 shows the coding of the samples.

X: The anatase content. Eq. 1

I_A: The peak intensity of (101) crystal planes associated with anatase. Eq. 1

I_R: The peak intensity of (101) crystal planes associated with rutile. Eq. 1

D: The crystallite size. Eq. 2

K: Scherrer constant equal to 0.89. Eq. 2

λ: The wavelength of incident ray. Eq. 2

β: The full width at half-maximum of the peak (FWHM). Eq. 2

θ: The plane peak position. Eq. 2

α: The fractional reflectance at each wavelength. Eq. 3

h: The Planck constant. Eq. 3

ν: The photon frequency. Eq. 3

Δθ: The hydrophilicizing rate ($deg.min^{-1}$) Table 5

Table 1. The coding of the samples.

Sample code	Composition			Calcination temperature
	Titania	Ce/Ti (%)	N/Ti (%)	(°C)
T	pure	0	0	550
0N-C-T	Ce doped titania	1	0	550
0.25N-C-T	N, Ce co-doped titania	1	0.25	550
0.5N-C-T	N, Ce co-doped titania	1	0.5	550
1N-C-T	N, Ce co-doped titania	1	1	550
2N-C-T	N, Ce co-doped titania	1	2	550

3- Results and discussion

3-1- XRD analysis

The XRD patterns of pure and N, Ce co-doped titania nanoparticles are shown in Figure 1. The located peaks at 2□: 25.3° and 27.4°, correspond to anatase (101) and rutile (110) crystal planes, respectively.

The results suggest that only anatase peak was detected in the N, Ce co-doped titania samples, while pure titania sample has both anatase and rutile peaks. The XRD patterns of the samples indicate that no characteristic peaks of nitrogen and cerium species were detected. This is may be attributed to the fact that the nitrogen and cerium species are present as a highly dispersed state in titania. Furthermore, the peak position shifts confirm the nitrogen and cerium co-doping into titania crystalline lattice [18, 19]. Comparison of the approximate anatase content and the average crystallite sizes were calculated by using equations 1 and 2 (Eq. 1 and 2) [20, 21] and are shown in Table 2.

$$X\,(\%) = 100/\,(1 + 1.256\,(I_R/I_A)) \quad \text{Eq. 1}$$

$$D = K\lambda/\beta\cos\theta \quad \text{Eq. 2}$$

According to the results, in pure titania sample the anatase content was about 72.9 %, and with increasing N/Ti doping ratio to 0.25%, the percentage of anatase phase has increased up to about 93.1%. While, when the N/Ti doping was increased to 2%, the anatase content has been reduced. On the other hand, it is obvious that increasing N/Ti doping ratio to 2%, reduces the crystallite size (from 27.2 nm to 10.7 nm). The results suggest that nitrogen and cerium doping into titania lattice postpones phase transformation from anatase to rutile and prevents the extreme growth of crystallite size. Since the ionic radius of Ce^{3+} and Ce^{4+} are larger than that of Ti^{4+}, it is difficult for Ce^{4+} to enter theTiO_2 crystalline lattice instead of Ti^{4+}. The

Ce^{3+} and Ce^{4+} ions seem more perhaps to become complex with the surface oxygen of TiO_2, which represses the growth of titania crystallite [22, 23].

3-2- AFM analysis

Figures 2 and 3 show the AFM images (three dimensional surface plots (1.0×1.0 μm^2)) and the AFM surface profile of samples, respectively. The particle size distribution and the roughness values of the pure and N, Ce co-doped titania coatings are summarized in Table 3.

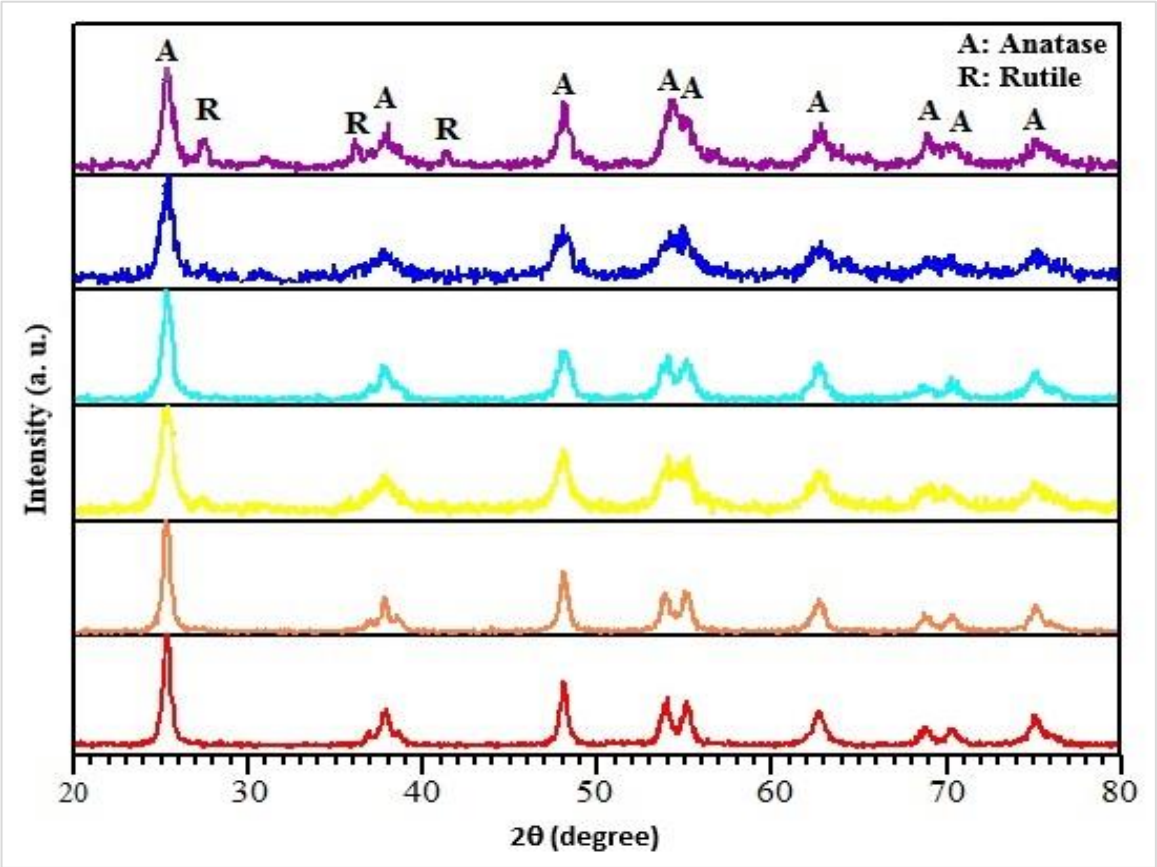

Fig. 1. XRD patterns of the pure and N, Ce co-doped titania nanoparticles.

Table 2. Crystalline properties of the pure and N, Ce co-doped titania nanoparticles.

Sample	Anatase content (%)	Average Anatase crystallite size (nm)
T	≅ 72.92	≅ 27.2
0N-C-T	≅ 86.53	≅ 19.2
0.25N-C-T	≅ 93.10	≅ 14.6
0.5N-C-T	≅ 86.67	≅ 12.7
1N-C-T	≅ 90.51	≅ 11.7
2N-C-T	≅ 91.51	≅ 10.9

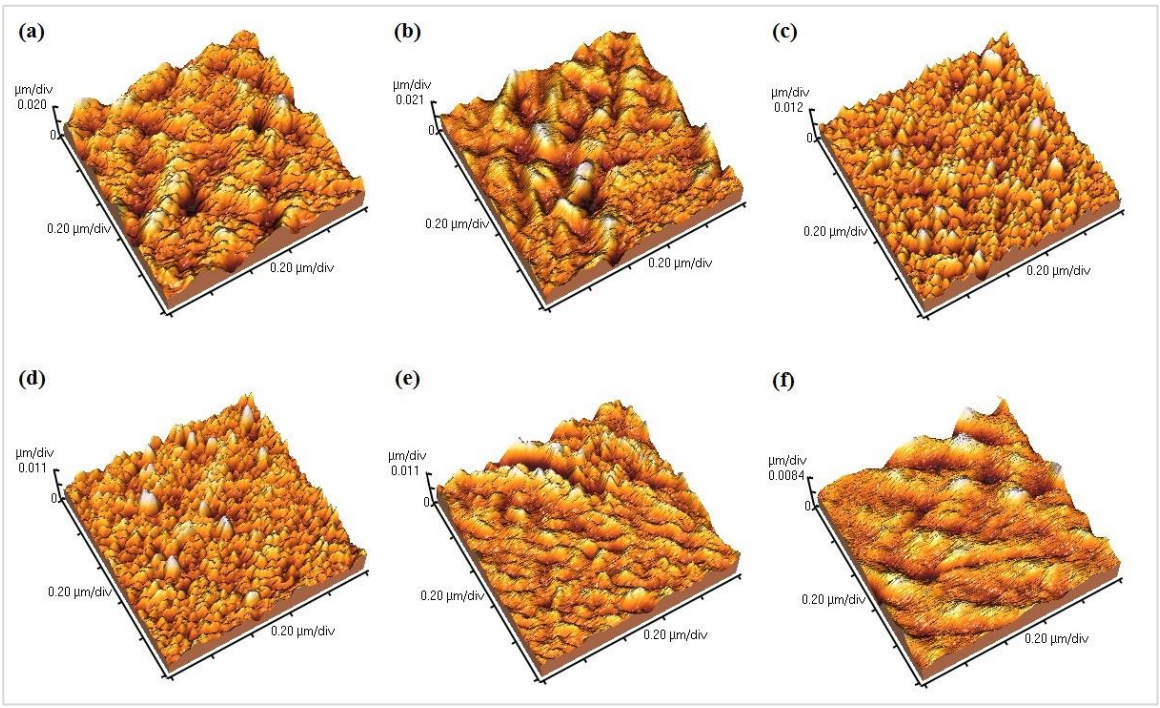

Fig. 2. AFM (3D) images of the pure and N, Ce co-doped titania coatings, a) T, b) 0N-C-T, c) 0.25N-C-T, d) 0.5N-C-T, e) 1N-C-T, f) 2N-C-T.

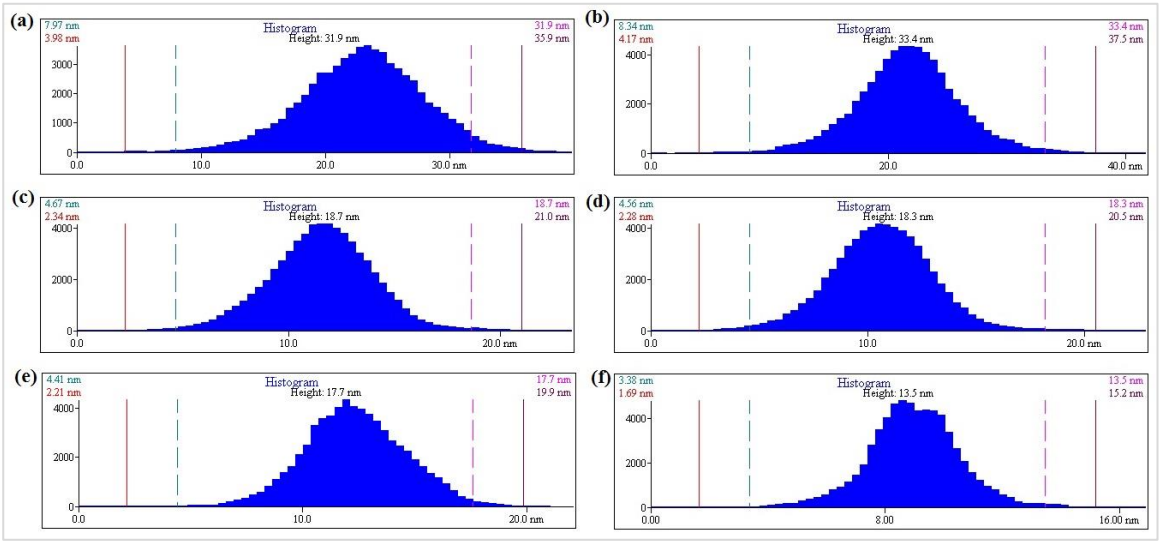

Fig. 3. AFM surface profile analysis of the pure and N, Ce co-doped titania coatings, a) T, b) 0N-C-T, c) 0.25N-C-T, d) 0.5N-C-T, e) 1N-C-T, f) 2N-C-T.

According to this results, the preparation of samples in nanoscale size are confirmed. On the other hand, with increasing nitrogen doping in co-doped titania samples, the average particle size and the surface roughness have been decreased. That is, N and Ce co-doping not only has prevented the growth of crystallites (according to the results of Table 2), but also has controlled the growth of particles. But in "1N-C-T" and "2N-C-T" samples that contain more urea and more doped nitrogen, nanoparticle agglomeration is observed, which reduces specific surface area and useful surface properties, and the lowest agglomeration is found in "0.25N-C-T" and "0.5N-C-T" samples.

3-3- DRS analysis

The diffuse reflectance spectroscopy of the pure and co-doped titania nanoparticles are presented in Figure 4a.

The shift in the absorption edge toward red wavelengths and a higher width are obvious in the N, Ce co-doped titania nanoparticles in comparison with pure titania nanoparticles. Furthermore, the co-doped titania samples relative to pure titania sample have higher light absorption in the visible range, and the widest absorption edge in the visible range is for "0.25N-C-T" sample. It seems the red-shift and higher light absorption are due to the presence of new energy level into the band gap, the energy level for Ce^{3+}/Ce^{4+} is 1.8 eV. [20]. Moreover, it is reasonable to consider that when amount of O atoms is replaced by N atoms in titania lattice, it creates a new energy level on top of the valance band and causes the red-shift [15, 24]. As a result, the widest absorption edge and highest light absorption in the visible range is for "0.25N-C-T" sample.

Kubelka-Munk function ($(\alpha h\nu)^{1/2}$ vs. $h\nu$ plots, Eq. 3 [25-27]) and the calculated band gaps of the samples are represented in Figure 4b and Table 4. According to the results, the observed band gaps for N, Ce co-doped titania nanoparticles are significantly lower than calculated value for pure titania nanoparticles (≅ 3.2 eV). As the N/Ti ratio increased to 0.25%, the band gap values of the samples have been decreased, but further increase of the N/Ti ratio and over-doping of titania nanoparticles, have increased the amounts of the bond gap, again. The remarkable thing is that all of the bond gap values of the co-doped titania samples are less than the value in the pure titania sample.

It can be concluded that nitrogen and cerium co-doping into titania lattice has decreased the band gap values, due to the creation of defect energy levels within titania [3, 15]. On the other hand, since in anatase phase, the indirect band gap is more effective and the lifetime of electron-hole pair is longer, the anatase phase has better photoelectric properties than the rutile phase [28, 29]. Eventually, "0.25N-C-T" sample (with maximum anatase content and the optimal doped value) has the smallest band gap of about 2.78 eV.

Table 3. Particle size distribution and roughness values of the pure and N, Ce co-doped titania coatings.

Sample	Particle size distribution (nm)	Average particle size (nm)	Average roughness (Ra) (nm)
T	≅ 7.97 – 31.9	22.94	3.880
0N-C-T	≅ 8.34 – 33.4	21.65	3.385
0.25N-C-T	≅ 4.67 – 18.7	11.53	1.916
0.5N-C-T	≅ 4.56 – 18.3	10.65	1.851
1N-C-T	≅ 4.41 – 17.7	12.31	1.789
2N-C-T	≅ 3.38 – 13.5	9.95	1.217

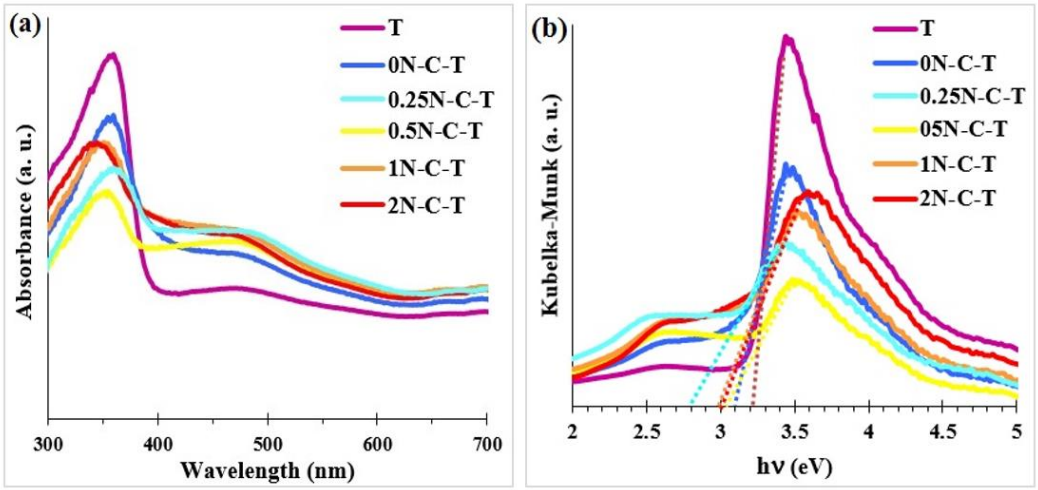

Fig. 4. (a) DRS, (b) Band gap determination of the pure and N, Ce co-doped titania nanoparticles.

Table 4. Values of band gap of the pure and pure and N, Ce co-doped titania nanoparticles.

Sample	T	0N-C-T	0.25N-C-T	0.5N-C-T	1N-C-T	2N-C-T
Band gap (eV)	≅ 3.21	≅ 3.1	≅ 2.78	≅ 3.03	≅ 2.98	≅ 3

3-4- Hydrophilicity analysis

Figures 5 and 6 show the water contact angle of the pure and N, Ce co-doped titania coatings under light irradiation in ambient conditions. After holding the specimens in dark conditions for 24 hours, the contact angles of the specimen surface have been measured about 62 to 79 degrees. Because the surface defective sites can be replaced by oxygen atoms and the surface wettability changes from hydrophilic to hydrophobic. After 20 and 40 min, visible light irradiation, the contact angles of all coatings decreased. That is, all samples have photo-induced hydrophilic property. As expected, "0.25N-C-T" sample showed the best photo-induced super-hydrophilicity. Its contact angle reduced from about 69° to less than 5° within 40 min, while the photo-induced hydrophilicity of pure titania coatings showed the worst case (reduction from about 79° to 38° within 40 min). For further quantitatively characterization, the photo-induced hydrophilicizing rates ($\Delta\theta$: deg.min^{-1}) of the coatings in 40 min under light radiation were compared. The hydrophilicizing rate of the coatings is summarized in Table 5. The difference in photo-induced hydrophilicizing rate of the coatings is related to the change in phase structure, surface topography, specific surface area and photoelectric properties [30, 31]. The hydrophilicizing rate ($\Delta\theta$) of "0.25N-C-T" is about 1.6 (deg.min^{-1}), while that of pure titania sample is just 1.01 (deg.min^{-1}).

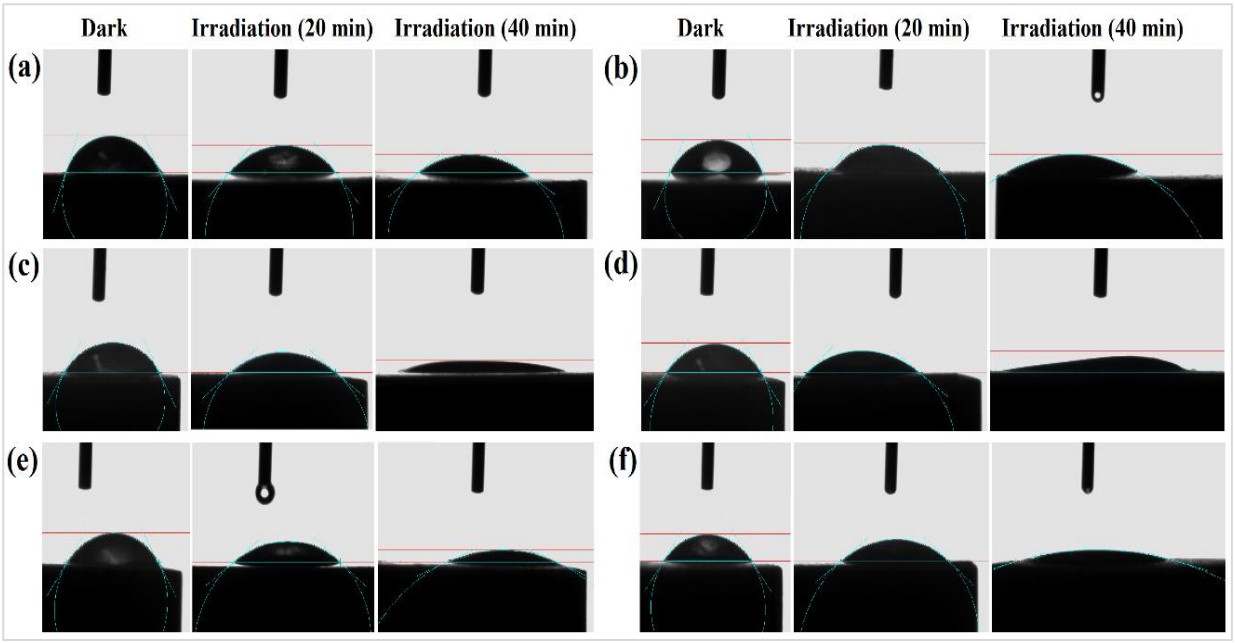

Fig. 5. The water contact angle of a) T, b) 0N-C-T, c) 0.25N-C-T, d) 0.5N-C-T, e) 1N-C-T, and f) 2N-C-T coatings under dark and light irradiation (20 and 40 min) conditions.

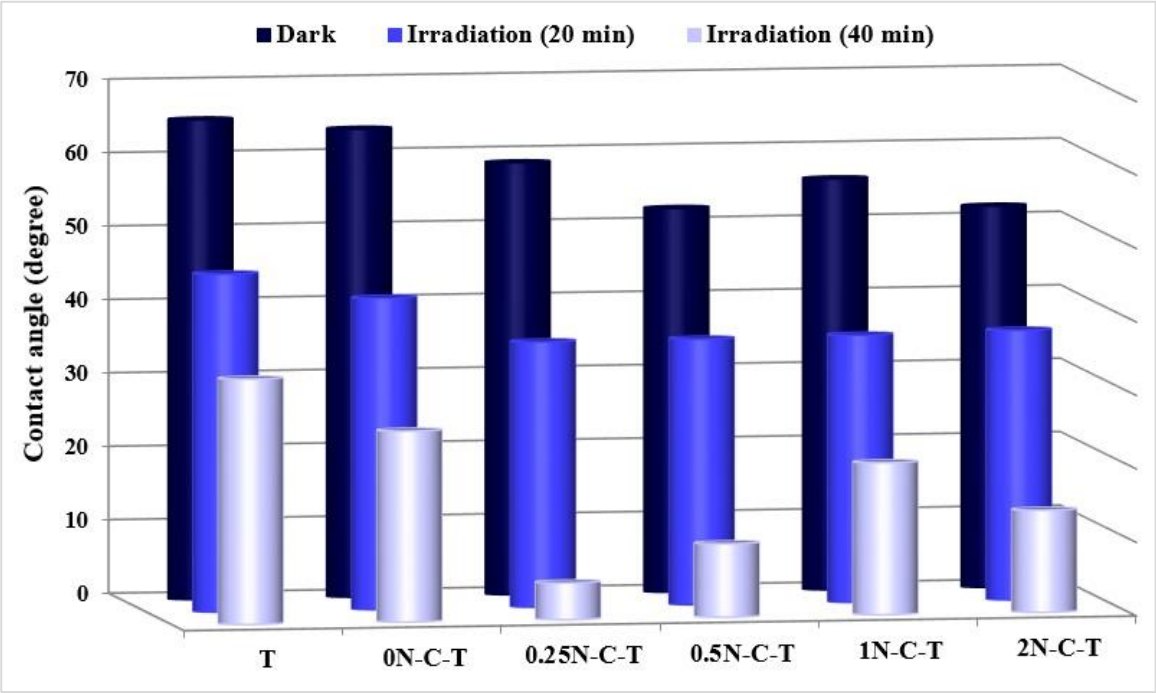

Fig. 6. The water contact angle of pure and N, Ce co-doped titania coatings under dark and light irradiation (20 and 40 min) conditions.

Table 5. Values of the hydrophilicizing rate of the pure and N, Ce co-doped titania coatings.

Sample	T	0N-C-T	0.25N-C-T	0.5N-C-T	1N-C-T	2N-C-T
hydrophilicizing rate ($\Delta\theta$) ($deg.min^{-1}$)	≅ 1.01	≅ 1.19	≅ 1.60	≅ 1.30	≅ 1.13	≅ 1.2

According to the following equations, titania irradiation causes the excitation of the electron-hole pair and leads to TiO_2 reduction from Ti^{4+} to Ti^{3+}, and oxygen vacancies are created on surface. Thus, H_2O molecules are adsorbed on defect positions to create a hydrophilic surface [15, 32, 33].

$TiO_2 + h\nu \rightarrow e^- + h^+$

$Ti^{4+} + e^- \rightarrow Ti^{3+}$

$Ti^{3+} + O_2 \rightarrow Ti^{4+} + O_2^-$

$O_2^- + h^+ \rightarrow O_2 + V_O$

In addition, the presence of N and Ce in titania structure can improve the photo-induced hydrophilic property, because N and Ce co-doping has reduced crystallite size of co-doped titania nanoparticles, results in, has increased the specific surface area (Table 3). Since the rate of hydrophilicity of rutile under irradiation is slower than that of anatase [32], and according to XRD results, it was observed that N, Ce co-doping in the titania structure results in increasing the percentage of anatase phase. Therefore, the photo-induced hydrophilicity of the co-doped titania samples has been increased. Moreover, N and Ce co-doping has improved the photoelectric properties of the samples, such as decreasing band gap values and increasing visible light absorption [according to Figure 4 and Table ٤]. And cerium acts as an electron trap and increases the lifetime of photo-generated electrons and holes in titania structure and creates more hydroxyl content on the surface (according to the following equations), which would also decrease the water contact angle [15, 34].

$Ce^{4+} + e^- \rightarrow Ce^{3+}$

$Ce^{3+} + O_2 \rightarrow Ce^{4+} + O_2^-$

$H_2O + h^+ \rightarrow OH° + H^+$

$O_2^- + H^+ \rightarrow OH°$

4- Conclusions

The pure and N, Ce co-doped titania nanoparticles were synthesized by sol-gel method. Then, the surface GCE was coated by the nanoparticles. The nanoparticles and coatings were characterized to investigate the effect of nitrogen doping amounts on the hydrophilic and photoelectric properties. The results of the XRD and AFM analyzes showed that N and Ce doping into titania lattice has delayed the transformation of anatase to rutile phase and has prevented the excessive growth of crystallites. In addition, the co-doping has reduced the surface roughness and the growth of surface particles. The study of the photoelectric behaviors of the nanoparticles showed that the N and Ce co-doped titania samples compared to the pure titania had the wider absorption edges and the higher light absorption values in visible range. And the band gap of the co-doped titania have also been reduced due to the creation of new energy levels by nitrogen and cerium in the band gap of titania. The results of the photo-induced hydrophilicity test also showed that all the samples are hydrophilic and N, Ce co-doping has improved the hydrophilicity, because the co-doping has modified the surface properties (increasing of the specific surface area and decreasing of the surface roughness), and has enhanced the photoelectric properties under visible irradiation (greater light absorption, Smaller band gap and longer electron-hole pair lifetime). Finally, it can be concluded that the optimum doping values of nitrogen and cerium are (N/Ti: 0.25%) and (Ce/Ti: 1%), respectively. And the sample containing these amounts of dopants has the highest percentage of anatase phase (93.1%) and the average crystallite size of about 14.6 nm and the surface roughness as about 1.91 nm. as well as it has the smallest band gap (2.78 eV) and highest super-hydrophilicizing rate (1.6 deg.min^{-1}). It seems can be a good composition for the modification of GCE surface in photoelectrochemical applications.

References:

[1] O. Carp, C.L. Huisman, A. Reller, "Photoinduced reactivity of titanium dioxide", Prog. Solid State Chem., Vol. 32, 2004, pp. 33-177.

[2] X. Chen, S.S. Mao, "Titanium Dioxide Nanomaterials: Synthesis, Properties, Modifications, and Applications", Chem. Rev., Vol. 107, 2007, pp. 2891-2959.

[3] N. Ahmadi, A. Nemati, M. Bagherzadeh, "Synthesis and properties of Ce-doped TiO_2-reduced graphene oxide nanocomposite", J. Alloys Compd., Vol. 742, 2018, pp. 986-995.

[4] S. Khosroyar, A. Arastehnodeh, "Improving hydrophilic and antimicrobial properties of membrane by adding nanoparticles of titanium dioxide and copper oxide", Membrane Water Treatment, Vol. 9, 2018, pp. 481-487.

[5] J. Moma, J. Baloyi, Modified Titanium Dioxide for Photocatalytic Applications, Photocatalysts - Applications and Attributes, S. B. Khan, K. Akhtar, IntechOpen. 2018.

[6] M, Nischk, P. Mazierski, Z. Wei, K. Siuzdak, N. A. Kouame, E. Kowalska, H. Remita, A. Zaleska-Medynska, "Enhanced photocatalytic, electrochemical and photoelectrochemical properties of TiO_2 nanotubes arrays modified with Cu, AgCu and Bi nanoparticles obtained via radiolytic reduction", Appl. Surf. Sci., Vol. 38, 2016, pp. 7:89–102.

[7] J. Bai, B. Zhou, "Titanium Dioxide Nanomaterials for Sensor Applications", Chem. Rev., Vol. 114, 2014, pp. 10131-10176.

[8] F. Hoseinian-Maleki, A. Nemati, F.J. Yasir, "Synthesis of C–N–Y tri-doped TiO_2 photo-catalyst for MO degradation and characterization", Mater. Res. Express, Vol. 2, 2015, pp. 105011.

[9] V. Štengl, S. Bakardjieva, N. Murafa, "Preparation and photocatalytic activity of rare earth doped TiO_2 nanoparticles", Mater. Chem. Phys., Vol. 114, 2009, pp. 217-226.

[10] M. M. Rashad, A. E. Shalan, M. Lira-Cantu, M. S. A. Abdel-Mottaleb, "Enhancement of TiO_2 nanoparticle properties and efficiency of dye-sensitized solar cells using modifiers", Appl. Nanosci., Vol. 3, 2013, pp 167–174.

[11] J. Low, J. Yu, M. Jaroniec, S. Wageh, A. A. Al-Ghamdi, "Heterojunction Photocatalysts", Adv. Mater., Vol. 29, 2017, pp. 1601694.

[12] F.T. Johra, W.G. Jung, "RGO-TiO_2-ZnO composites: Synthesis, characterization, and

application to photocatalysis", Appl. Catal. A: Gen., Vol. 491, 2015, pp. 52-57.
[13] H. Shi, T. Zhang, T. An, B. Li, X. Wang, "Enhancement of photocatalytic activity of nano-scale TiO_2 particles co-doped by rare earth elements and heteropolyacids", J. Colloid Interface Sci., Vol. 380, 2012, pp. 121-127.
[14] I. Cacciotti, A. Bianco, G. Pezzotti, G. Gusmano, "Synthesis, thermal behaviour and luminescence properties of rare earth-doped titania nanofibers", Chem. Eng. J., Vol. 166, 2011, pp. 751-764.
[15] N. Ahmadi, A. Nemati, M. Solati-Hashjin, "Synthesis and characterization of co-doped TiO_2 thin films on glass-ceramic", Mater. Sci. Semicond. Process., Vol. 26, 2014, pp. 41–48.
[16] B. Viswanathan, K. R. Krishanmurthy, "Nitrogen Incorporation in TiO_2: Does It Make a Visible Light Photo-Active Material?", Int. J. Photoenergy, vol. 2012, 2012, pp. 269654.
[17] E. M. Samsudin, S. B. A. Hamid, J. C. Juan, W. J. Basirun, A. E. Kandjanib, S. K. Bhargavab, "Controlled nitrogen insertion in titanium dioxide for optimal photocatalytic degradation of atrazine", RSC Adv., Vol. 5, 2015, pp. 44041-44052.

[18] Z. Liu, B. Guo, L. Hong, H. Jiang, "Preparation and characterization of cerium oxide doped TiO_2 nanoparticles", J. Phys. Chem. Solids, Vol. 66, 2005, pp. 161-167.
[19] V. Caratto, L. Setti, S. Campodonico, M. M. Carnasciali, R. Botter, M. Ferretti, "Synthesis and characterization of nitrogen-doped TiO_2 nanoparticles prepared by sol–gel method", J. Sol-Gel Sci. Technol., Vol. 63, 2012, pp. 16-22.
[20] Y. Xu, H. Chen, Z. Zeng, B. Lei, "Investigation on mechanism of photocatalytic activity enhancement of nanometer cerium-doped titania", Appl. Surf. Sci., Vol. 252, 2006, pp. 8565-8570.
[21] L. Luo, T. Li, X. Ran, P. Wang, L. Guo, "Probing photocatalytic characteristics of Sb-Doped TiO_2 under visible light irradiation", J. Nanomater., Vol. 2014, 2014, pp. 8.
[22] C. Liu, X. Tang, C. Mo, Z. Qiang, "Characterization and activity of visible-light-driven TiO_2 photocatalyst codoped with nitrogen and cerium", J. Solid State Chem., Vol. 181, 2008, pp. 913-919.
[23] T. Tsoncheva, A. Mileva, G. Issa, M. Dimitrov, D. Kovacheva, J. Henych, N. Scotti, M. Kormunda, G. Atanasova, V. Stengl, "Template-assisted hydrothermally obtained titania-ceria composites and their application as catalysts in ethyl acetate oxidation and methanol decomposition with a potential for sustainable environment protection", Appl. Surf. Sci., Vol. 396, 2017, pp. 1289-1302.
[24] T. Yu, X. Tan, L. Zhao, Y. Yin, P. Chen, J. Wei, "Characterization, activity and kinetics of a visible light driven photocatalyst: Cerium and nitrogen co-doped TiO_2 nanoparticles", Chem. Eng. J., Vol. 157, 2010, pp. 86-92.
[25] S. Khanchandani, S. Kumar, A.K. Ganguli, "Comparative Study of TiO_2/CuS Core/Shell and Composite Nanostructures for Efficient Visible Light Photocatalysis", ACS Sustainable Chem. Eng., Vol. 4, 2016, pp. 1487-1499.
[26] R. López, R. Gómez, "Band-gap energy estimation from diffuse reflectance measurements on sol–gel and commercial TiO_2: a comparative study", J. Sol-Gel Sci. Technol., Vol. 61, 2012, pp. 1-7.
[27] B. Choudhury, M. Dey, A. Choudhury, "Defect generation, d-d transition, and band gap reduction in Cu-doped TiO_2 nanoparticles", Int. Nano Lett., Vol. 3, 2013, pp. 1-8.
[28] J. Zhang, P. Zhou, J. Liu, J. Yu, "New understanding of the difference of photocatalytic activity among anatase, rutile and brookite TiO_2", Phys. Chem. Chem. Phys., Vol. 16, 2014, pp. 20382-20386.
[29] T. Zhu, S. P. Gao, "The Stability, Electronic Structure, and Optical Property of TiO_2 Polymorphs", J. Phys. Chem., Vol. 118, 2014, pp. 11385-11396.
[30] F. Meng, Z. Sun, "A mechanism for enhanced hydrophilicity of silver nanoparticles modified TiO_2 thin films deposited by RF magnetron sputtering", Appl. Surf. Sci., Vol. 255, 2009, pp. 6715-6720·
[31] Bayati, R. Molaei, A. Kajbafvala, S. Zanganeh, H. R. Zargar, K. Janghorban, "Investigation on hydrophilicity of micro-arc oxidized TiO_2 nano/micro-porous layers", Electrochim. Acta, Vol. 55, 2010, pp. 5786–5792.
[32] J. C. Yu, J. Yu, W. Ho, J. Zhao, "Light-induced super-hydrophilicity and photocatalytic activity of mesoporous TiO_2 thin films", J.

Photochem. Photobiol., A, Vol. 148, 2002, pp. 331-339.

[33] T. Shibata, G. Takanashi, T. Nakamura, K. Fukuda, Y. Ebinad, T. Sasaki, "Titanoniobate and niobate nanosheet photocatalysts: superior photoinduced hydrophilicity and enhanced thermal stability of unilamellar Nb_3O_8 nanosheet", Energy Environ. Sci., Vol. 4, 2011, pp. 535-542.

[34] L. Zhao, Q. Jiang, J. Lian, "Visible-light photocatalytic activity of nitrogen-doped TiO_2 thin film prepared by pulsed laser deposition", Appl. Surf. Sci., Vol. 254, 2008, pp. 4620-4625.